PHASE-RESOLVED OBSERVATIONS OF THE SOFT X-RAY INTERMEDIATE POLAR RXJ0558.0+5353*

D. de Martino[1], M. Mouchet[2], J.M. Bonnet-Bidaud[3]

[1]Osservatorio Astronomico di Capodimonte, I-80131, Naples, Italy
[2]DAEC, Observatoire de Paris-Meudon, F-92190 Meudon, France
[3]Service D'Astrophysique, CEN, F-91191 Gif-Sur-Yvette, France

ABSTRACT

First IUE observations of the newly discovered soft X-ray Intermediate Polar RX J0558.0+5353 are presented together with coordinated optical low resolution spectroscopy. The UV spectrum, is similar to those observed in other "hard" IPs, though sharing some characteristics of Polars. We find a weak UV orbital variability in the continuum and lines. Optical emission lines display low-amplitude orbital radial velocity variations whose phasing, if interpreted as the motion of material circulating around the white dwarf, implies that the UV continuum modulation originates in the hot-spot, corresponding to the impact region of the accretion flow onto a ring/disc. A relatively hot temperature is derived for the orbital modulated UV continuum, un-typical for "standard" CV hot-spots.

Key words: X-rays: binaries; Stars: Cataclysmic Variables; Stars: individual: RX J0558.0+5353.

1. INTRODUCTION

Intermediate Polars (IPs) are asynchronous ($P_{rot} < P_{orb}$) binary systems containing a magnetized white dwarf (B $<$ 10 MG) accreting material from a late type main sequence star. IPs are variable on different timescales and in all energy regimes (Patterson 1994). The study of periodicities like the rotational, the orbital and beat periods simultaneously on a wide energy range is a powerful tool in inferring the accretion geometry in these binaries. Differently from the synchronous AM Her type (or Polars) magnetic Cataclysmic Variables (mCVs), IPs are typically " hard " X-ray emitters. The recent ROSAT survey has revealed few unprecedented IPs possessing a substantial soft X-ray emission (Mason et al. 1992; Haberl et al. 1994), among them the source RX J0558.0+5353 (hereafter RX0558) recently identified by Haberl et al. (1994). Its X-ray emission is relatively soft (kT $\sim$ 50 eV) and dominated by a 272 s modulation, identified as the first harmonic of the rotational 545 s period of the white dwarf (Haberl & Motch 1995; Ashoka et al. 1995; Skillman 1996; Allan et al. 1996). Only very recently it has been discovered to possess a spin modulated circular optical polarization, but with the first harmonic dominating the un-polarized optical flux (Shakhovskoi & Kolesnikov 1997). The detection of modulated polarized light makes this system the third IP, together with PQ Gem and RX J1712.6-2414, sharing this typical property of Polars. We also note that although BG CMi is a polarized IP, its polarization is not spin modulated. All this suggests that these few apparently "true" interpolars might be progenitors of the synchronous systems (cfr. Mouchet et al., this proceedings (henceforth MBBDM)).

Optical follow-up observations revealed low amplitude radial velocity variations of Balmer and He II lines at the most likely 4.15 hr binary period (Haberl et al. 1994). This determination of the orbital period allowed us to perform UV IUE observations in the framework of our program aiming to study UV properties of IPs and to detect eventual orbital variability. Given the variable nature of these systems, the IUE observations were complemented with coordinated optical spectroscopy acquired at OHP observatory.

2. OBSERVATIONS AND AVERAGE SPECTRAL PROPERTIES

IUE observations were carried out on Feb. 7 1996, from 05:25 UT to 20:47 UT during the 19th IUE episode using continous 16 hr observing time. SWP and LWP cameras have been exposed in low dispersion mode and with the large aperture for multiple of the 272 s optical photometric period. A total of 9 SWP and 8 LWP images have been acquired with an orbital phase resolution between 0.16 (LWP) and 0.24 (SWP).

Optical low resolution (15-20 Å) spectroscopy in the 3640-7100 Å range was carried out on Feb. 11-15 1996 at OHP observatory using the 1.93 m telescope equipped with the Carelec/TK CCD spectrograph configuration. A total of 87 spectra have been acquired during the 4 nights with exposure times twice

*Based on IUE observations collected at VILSPA ESA Satellite Tracking station, Madrid, Spain

or three times the photometric period, resulting in an orbital phase resolution between 0.037 and 0.055.

The grand average UV spectrum, shown in Fig. 1, is typical of both IPs and Polars with a relatively flat continuum and with the typical strong emission lines of NV, SiIV, CIV and HeII. Weaker emissions of SiIII/SiII/OI (1298/1304/1305 Å), CIII (1175 Å), CII (1335 Å), AlII (1670 Å), AlIII (1857 Å), CIII/HeII (2300 Å) and HeII (2307,2386 Å) as well as Mg II (2800 Å) are also detected. The presence of a wide range of ionization states appears to be a common characteristic of Polars rather than IPs (de Martino 1995a, 1995b, these proceedings), which makes RX0558 more similar to the synchronous systems rather than to its class analogues. This property is also shared by the other two Polar progenitor candidates PQ Gem and RX J1712.6-2414 (see MBBDM). However, line flux ratios of NV:SiIV:CIV:HeII fall within the observed range for IPs (see also MBBDM and de Martino, this proceedings).

Also the optical spectrum is typical of mCVs with strong Balmer, HeII and HeI lines. H_β is similar in strength to HeII (4686 Å) similarly to the other IP FO Aqr. The presence of FeII line at 5169 Å detected by Haberl et al. (1994) is also confirmed. Line ratios are H_β : H_α : H_γ : HeII (4686 Å): HeII (5411 Å) = 1:1.57:0.83:0.99:0.14.

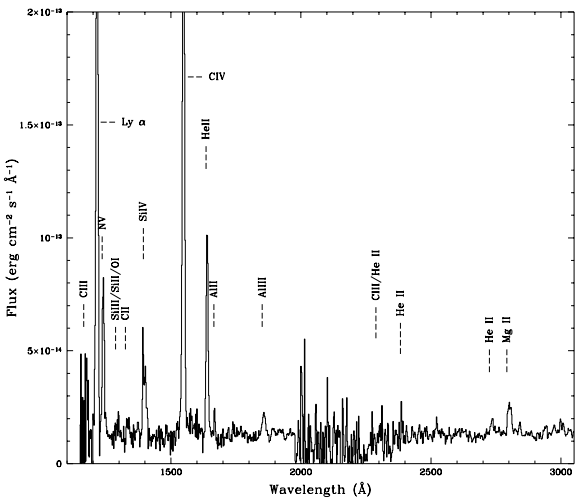

Figure 1. Grand average UV spectrum of RX0558 together with emission line identification.

The IUE spectrum appears to be affected by the interstellar absorption feature at 2200 Å from which $E_{B-V} = 0.12 \pm 0.05$ is derived (see MBBDM for a detailed discussion of reddening). This is consistent with the hydrogen column density inferred from ROSAT data (Haberl & Motch 1995). We henceforth adopt a conservative value of $E_{B-V} = 0.1$. As outlined in Fig. 3 of MBBDM, the UV continuum to the emission line (NV,SiIV, CIV,HeII) dereddened flux ratio falls in the observed range of Polars rather than of IPs, this ratio being a good discriminator between Polars and IPs (see also de Martino, these proceedings).

3. THE ORBITAL VARIABILITY

3.1. The UV variability

We inspected continuum spectral variability by measuring broad band line free continuum fluxes in the following ranges: 1265-1275 Å, 1425-1510 Å, 1680-1710 Å, 1793-1825 Å, 1890-1960 Å, 2450-2700 Å, and 2860-2980 Å. A very weak modulation by a factor of $\sim 14\%$ is found in both far and near-UV, thus with no colour dependence. The SW and LW line free continuum light curves are presented in Fig. 3, where the maximum is found between orbital phases 0.0 and 0.2.

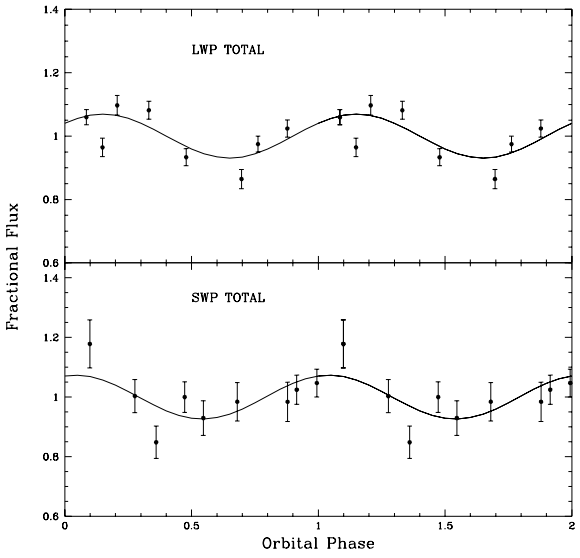

Figure 2. Folded far (bottom) and near-UV (top) continuum light curves using Haberl et al.'s (1994) ephemeris: T_0 = HJD 2449527.8275; P=0.17345 d, together with their best sinusoidal fits.

On the other hand, the major emission lines NV, SiIV, CIV and HeII, once inspected for orbital variability in their fluxes, equivalent widths (EWs) and violet-to-red (V/R) ratios do not show a clear orbital variability, except for an indication of line strengthening around orbital phase 0.

The spectrum of the orbital modulation has been derived from sinusoidal fits to the broad band continuum light curves as well as to the complete UV spectrum ones and is shown in Fig. 3,. Different spectral fits have been attempted. We did not include the optical modulation in the fits since the absolute flux calibration was inaccurate due to seeing problems. Best match in the UV is found with a black-body distribution at $T = 20000 \pm 1000$ K.

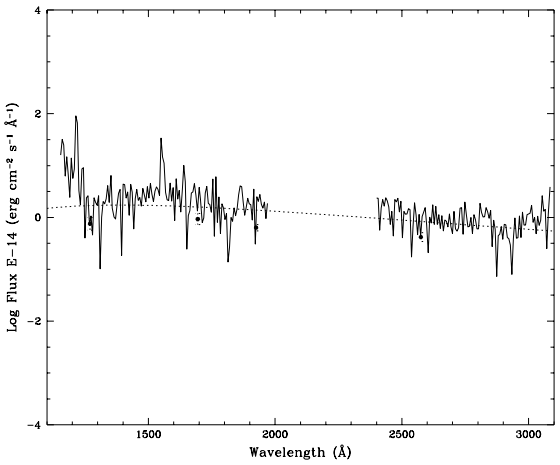

Figure 3. The spectrum of the UV orbital modulation together with the best black-body fit at 20000±1000 K. Points refer to the continuum broad band flux full-amplitudes.

3.2. Optical Radial Velocity Variations

Optical spectra have been folded in 11 bin phases corresponding to the UV orbital coverage and have been inspected for variability in their line fluxes, EWs and radial velocities. H_α, H_β and HeII (4686 Å) have been fitted with Gaussian profiles. For HeII a second component has been added redwards to account for the blend with HeI (4713 Å) line. As in the UV lines, no clear orbital variability is found in either line intensities or EWs, while a low-amplitude modulation is observed in their radial velocity curves, as also found by Haberl et al. (1994). We note that the accuracy of their ephemeris does not allow us to make direct comparison with our radial velocity variations but, differently from those results, we do not observe the phase lag between HeII (4686 Å) and H_α and H_β. The radial velocity parameters are listed in Table 1, where ϕ_0 refers to the blue-to-red crossing of emission lines.

Table 1. Radial velocity parameters

	H_α	H_β	HeII (4686 Å)
γ (km s^{-1})	9.1±1	-35 ± 1	-50±2
K (km s^{-1})	62±2	65±2	27±3
ϕ_0	0.854±0.003	0.791±0.004	0.860±0.016

4. DISCUSSION AND CONCLUSIONS

We have analyzed the first UV spectra of the soft X-ray IP RX0558, which show that, altough retaining the general characteristics of "hard" IPs, RXJ0558 shares UV similarities with the synchronous Polar systems. From these phase resolved IUE spectra we have inferred a weak continuum UV modulation by a factor of $\sim 14\%$ whilst emission lines are more erratic. Similar results in the EWs and line intensities of the optical emission lines from coordinated observations have been found. However low-amplitude optical radial velocity variations are indeed observed suggesting a low inclination system. Assuming that emission lines originate in a material moving circularly around the white dwarf, the blue-to-red crossing at $\Phi_{\rm orb} \sim 0.8$ (see Table 1) can be interpreted as the inferior conjunction of the primary star.

The spectrum of the UV orbital variability is compatible with a relatively hot component at T $\sim$ 20000 K. We derive a projected emitting area of $\sim 4 - 37 \cdot 10^{19}$ cm^2 for a distance range of 100-300 pc. This translates into a linear scale of $\sim 4 - 13\,{\rm R_{wd}}$ for a typical white dwarf radius of $8 \cdot 10^8$ cm, which is much smaller than the white dwarf Roche lobe radius for a 4.15 hr binary and a $1\,{\rm M_\odot}$ white dwarf.

As the phase of the maximum of the UV continuum variability lags by 0.3±0.1 in orbital phase the inferior conjunction of the white dwarf, in the standard accretion picture, this would correspond to the inferior conjunction of the hot-spot, the impact region of the accretion flow onto a disc or ring or onto the magnetosphere. In this respect RX0558, is different from FO Aqr and BG CMi, where the UV continuum modulation originates in the X-ray illuminated face of the hot-spot (bulge) (de Martino et al. 1994;1995; these proceedings). However, the intrinsic emission from a hot-spot located at the magnetospheric boundary is expected to emit in the X-ray regime as in the case of BG CMi (Norton et al. 1992). On the other hand, standard CV hot-spots are relatively cooler than our temperature estimate (Patterson 1994). A viable solution then appears if this region is located at the boundary of a ring, or a reduced disc not filling the white dwarf Roche lobe. Such partial discs can indeed be present in relatively strongly magnetized CVs (Hellier 1992) and the magnetic evidence in RX0558 might support this interpretation.

Further high temporal and spectral resolution observations in both UV and optical ranges are now needed to confirm and constrain the accretion geometry in this system.

ACKNOWLEDGMENTS

Part of this work was done when DdM was under ESA contract at the IUE Observatory VILSPA. The authors wish to express their gratitude to all ESA and INSA IUE VILSPA staff for their valuable help in the observing scheduling, observations and data processing.

REFERENCES

Allan A., Horne K., Hellier C. et al. 1996, MNRAS, 279, 1345.

Ashoka B.N., Marar T.M.K., Seetha S. et al. 1995, A&A, 297, L83.

de Martino D., Buckley D., Mouchet M. et al. 1994, A&A, 284, 125.

de Martino D., 1995a, in 'Cataclysmic Variables: interclass relations', eds. A. Bianchini, M. Della Valle, M. Orio, p397.

de Martino D., 1995b, in 'Cape Workshop on Magnetic Cataclysmic Variables', ASP Conf. Ser. 85, p238.

de Martino D., Mouchet M., Bonnet-Bidaud JM. et al. 1995, A&A, 298, 849.

Haberl F., Thorstensen J.R., Motch C. et al. 1994, A&A, 291, 171

Haberl F., Motch C., 1995, A&A 297, L37

Hellier C., 1992, MNRAS, 258,578.

Mason K.O., Watson M.G., Ponman T.J. et al. 1992, MNRAS, 258, 749

Norton A.J., McHardy I.M., Lehto H.J. et al. 1992, MNRAS, 258, 697.

Patterson J. 1994, PASP, 106, 209.

Shakhovskoi N.M. & Kolesnikov S.V. 1997, IAU Circ. 6760.

Skillman D.R. 1996, PASP, 108, 130.